The Journal of Neuroscience, April 1, 2001, 21(7):2288–2297

Changes in Microtubule Stability and Density in Myelin-Deficient Shiverer Mouse CNS Axons

Laura L. Kirkpatrick,[1] Andrea S. Witt,[1] H. Ross Payne,[1] H. David Shine,[2] and Scott T. Brady[1]

[1]Department of Cell Biology, University of Texas Southwestern Medical Center, Dallas, Texas 75235, and [2]Departments of Neurosurgery, Neuroscience, Molecular and Cellular Biology, Baylor College of Medicine, Houston, Texas 77030

Altered axon–Schwann cell interactions in PNS myelin-deficient Trembler mice result in changed axonal transport rates, neurofilament and microtubule-associated protein phosphorylation, neurofilament density, and microtubule stability. To determine whether PNS and CNS myelination have equivalent effects on axons, neurofilaments, and microtubules in CNS, myelin-deficient shiverer axons were examined. The genetic defect in shiverer is a deletion in the myelin basic protein (MBP) gene, an essential component of CNS myelin. As a result, shiverer mice have little or no compact CNS myelin. Slow axonal transport rates in shiverer CNS axons were significantly increased, in contrast to the slowing in demyelinated PNS nerves. Even more striking were substantial changes in the composition and properties of microtubules in shiverer CNS axons. The density of axonal microtubules is increased, reflecting increased expression of tubulin in shiverer, and the stability of microtubules is drastically reduced in shiverer axons. Shiverer transgenic mice with two copies of a wild-type myelin basic protein transgene have an intermediate level of compact myelin, making it possible to determine whether the actual level of compact myelin is an important regulator of axonal microtubules. Both increased microtubule density and reduced microtubule stability were still observed in transgenic mouse nerves, indicating that signals beyond synaptogenesis and the mere presence of compact myelin are required for normal regulation of the axonal microtubule cytoskeleton.

Key words: axonal transport; glia; oligodendrocyte; myelin; shiverer; microtubule

Vertebrates have two distinct paths for formation of compact myelin. CNS and PNS myelin serve comparable functions and are superficially similar, but they differ in embryonic origin, genetics, composition, and ultrastructure. In both CNS and PNS, myelination is a complex process in which glial cells extend processes that enwrap axons and generate compact myelin (Morell and Quarles, 1999). However, Schwann cells enwrap single axons in the PNS, whereas one oligodendrocyte myelinates 6–10 different axons in the CNS. Myelin protein composition also differs. For example, myelin basic protein (MBP) comprises up to 40% of oligodendrocyte protein synthesis but is much lower in PNS. Although proteins responsible for compaction of CNS and PNS myelin are well characterized, less is known about proteins mediating axon–glial cell interactions in either CNS or PNS. Equally important, neuronal responses to different CNS or PNS environments are virtually uncharacterized.

The neuronal cytoskeleton is critical for neurite outgrowth during development and regeneration (Brady, 1993). This cytoskeleton comprises microtubules (MTs), neurofilaments (NFs), and microfilaments. Hallmark changes in isotype composition, posttranslational modification, and stability of these accompany neuronal development and regeneration (Brady et al., 1984; Sahenk and Brady, 1987; Hoffman and Cleveland, 1988; Oblinger and Lasek, 1988; Tetzlaff et al., 1988; Oblinger et al., 1989; Tashiro and Komiya, 1991), but the consequences of these changes are unknown. Our previous studies on the dysmyelinating mutant Trembler demonstrated that myelinating glia can affect the axonal cytoskeleton (Witt and Brady, 2000). Trembler mice fail to maintain compact myelin (Suter et al., 1992), leading to decreased axonal caliber, increased cytoskeletal densities, reduced slow axonal transport rates, reduced phosphorylation of cytoskeletal proteins, and decreased MT stability (de Waegh and Brady, 1990, 1991; de Waegh et al., 1992; Kirkpatrick and Brady, 1994).

To investigate whether PNS and CNS myelination affects axons equivalently, we examined CNS myelin-deficient shiverer mice. Shiverer mice contain a deletion in the MBP gene, do not produce MBP protein, and have no compact CNS myelin (for review, see Readhead and Hood, 1990). Shiverers display an action tremor that becomes progressively more prominent, leading to seizures, a shortened life-span, increased slow axonal transport rates, and altered NF composition (Brady et al., 1999). Here we examine the effects of myelin on axonal MT composition, stability, and organization.

To determine whether changes in shiverer MTs resulted solely from the absence of compact myelin, we analyzed a transgenic model with two wild-type MBP transgenes in a shiverer background. Transgenic shiverer mice express only 25% of normal MBP levels, generating a thin functional compact myelin sheath (Shine et al., 1992) that virtually eliminates tremors and allows a normal life-span (Readhead et al., 1987). Studying transgenic shiverer mice permits distinctions between parameters affected by the presence of compact myelin and those requiring a full

Received June 14, 2000; revised Dec. 27, 2000; accepted Dec. 29, 2000.

This work was supported in part by National Institute of Neurological Disease and Stroke Grants NS23868 and NS23320, National Institute of Aging Grant AG12646, NASA Grant NAG2–962, and Welch Foundation Grant 1237. We thank Drs. Carol Readhead and Susan Billings-Gagliardi for making shiverer and shiverer transgenic mice available to us. We also thank Robin Wray, Zhao Min, and Milena Gould for their technical assistance.

Correspondence should be addressed to Dr. Scott Brady, University of Texas, Southwestern Medical Center, Department of Cell Biology, 5323 Harry Hines Boulevard L1.209, Dallas, TX 75390-9039. E-mail: Scott.Brady@UTSouthwestern.edu.

Dr. Kirkpatrick's current address: Department of Molecular and Human Genetics, Baylor College of Medicine, Houston, TX 77030.

Copyright © 2001 Society for Neuroscience 0270-6474/01/212288-10$15.00/0

complement of compact myelin. Our results demonstrate that signals attributable to myelinating glia regulate the axonal cytoskeleton and these signals change with levels of compact myelin.

MATERIALS AND METHODS

All chemicals used were American Chemical Society quality or better and were obtained from Sigma (St. Louis, MO), CalBiochem (San Diego, CA), or Polysciences (Warrington, PA). Male and female shiverer and MBP/MBP transgenic mice (4–6 weeks old; provided by Carol Readhead, Cedars Sinai Medical Center, Los Angeles, CA, and Dr. Susan Billings-Gagliardi, University of Massachusetts Medical School, Worchester, MA) were used for all experiments. Age-matched wild-type mice (B6C3/F1) were obtained from Jackson Laboratories (Bar Harbor, ME). All mice were kept in a sterile environment and fed sterile food and water throughout the experiments.

Axonal transport labeling and cold-calcium fractionation. Proteins carried by axonal transport in mouse optic nerve were labeled by the intraocular injection of 0.5 mCi of ^{35}S-methionine (Trans ^{35}S Label; ICN Biochemicals, Costa Mesa, CA) into the right eye as described previously (Brady, 1985). The injection apparatus consisted of a 30 gauge needle connected to a Hamilton syringe by a length of polyethylene tubing. Injection-sacrifice intervals (ISIs) were chosen to position the peak of the Slow Component (SC)a (18–24 d) or SCb (4–7 d) wave fully in the optic nerve–optic tract.

To facilitate comparison of transport rates of proteins in different animals, the total amount of radioactivity in optic nerve segments was summed, and the cumulative amount of radioactivity in sequential segments was measured. The segment containing the 50% point of radioactivity was identified, and the distance of the 50% point from cell bodies was divided by the ISI to estimate the average rate of movement in a given nerve (Hoffman et al., 1983). Data for all nerves at a given ISI range were averaged, and the statistical significance of rate differences was determined by a two-sample *t* test using Data Desk software. Data are expressed as the mean ± SEM.

For cold-calcium tubulin experiments, optic nerves labeled with SCa were removed and homogenized in 500 μl of ice-cold MTG buffer containing 1 mM EGTA, 0.5 mM $MgCl_2$, 1 mM GTP, and protease inhibitors in 0.1 M MES, pH 6.8, using ground-glass microhomogenizers. After a 30 min incubation on ice, the homogenate was centrifuged at 120,000 × *g* (30 min, 4°C). The resulting supernatant (S1) contained cold-soluble proteins and was TCA precipitated. This first pellet (P1) was resuspended in an equal volume of CMTG buffer containing 5 mM $CaCl_2$, 0.5 mM $MgCl_2$, 1 mM GTP, and protease inhibitors in 0.1 M MES, pH 6.8, at room temperature, incubated 30 min, and then centrifuged at 120,000 × *g* (30 min, 25°C). The resulting supernatant (S2) contained cold-insoluble, calcium-soluble proteins, and was also TCA-precipitated. The final pellet (P2) contained cold- and calcium-insoluble proteins. The P2 pellet and the TCA pellets were solubilized in 200 μl of BUST containing 2% β-mercaptoethanol, 8 M urea, 1% SDS, 0.1 M Tris, 0.02% phenol red, and 5 μl aliquots were counted for radioactivity. Equal volumes of S1, S2, and P2 were separated by SDS-PAGE on 4–16% (0–6 M urea) gradient gels. The gels were stained with Coomassie blue and destained, then treated for fluorography with DMSO (2 × 30 min) and PPO (22% in DMSO, 3 hr) (Laskey and Mills, 1975). Gels were then dried and exposed to preflashed x-ray film for the appropriate time. The amount of radioactivity incorporated into specific proteins was quantitated by excising the appropriate bands from gels using the fluorographs as a template. Bands were solubilized in 30% hydrogen peroxide for 2 d at 60°C and counted in a liquid scintillation counter.

For comparison between mouse types, the amount of radioactivity for a given protein in S1, S2, and P2 was summed, and each fraction was expressed as a percentage of the total. Statistically significant differences in P2 radioactivity were determined by a two-sample *t* test using Data Desk (Data Description, Ithaca, NY) software. To analyze the fraction of total SCa radioactivity represented by tubulin and NF subunits, the radioactivity values in all 13 bands and spaces cut from gels were summed (S1 + S2 + P2), and counts in tubulin or an NF were divided by this total. Significance was determined by a two-sample *t* test using Data Desk software. Four data points were collected for each mouse type.

Preparation of MT fractions and quantitative immunoblotting. Whole brains were collected from shiverer, transgenic, and wild-type mice and used to prepare MTs with the aid of Taxol. Protein concentrations were determined using the BCA assay (Pierce, Rockford, IL), and equal amounts of total MT protein were run on gradient SDS-PAGE gels. Proteins were transferred to Immobilon-P transfer membrane (Millipore, Bedford, MA) for 18–20 hr at 25 V in transfer buffer containing 0.0125 M Tris, 0.096 M glycine, 0.1% SDS, pH 8.6. Blots were blocked for 1.5–2 hr in blocking buffer containing 6% casein, 1% PVP-40, 10 mM EDTA, in PBS, pH 7.4, then reacted with primary antibody diluted in blocking buffer for 2–4 hr. Primary antibodies used in these studies include Tu27, a total β-tubulin monoclonal antibody (generously provided by Dr. A. Frankfurter, University of Virginia) (Caceres et al., 1984) and DM1A, a total α-tubulin monoclonal antibody (Sigma). After three washes in 0.3% Tween 20 in PBS (PBST), blots were incubated in secondary antibody diluted in blocking buffer for 2 hr. For quantitative immunoblots, secondary antibody was rat anti-mouse IgG (Jackson ImmunoResearch, West Grove, PA) used at 1:1000. After another round of washing in PBST, the blots were incubated in ^{125}I-Protein A (1 μCi/10 ml of blocking buffer; Amersham Pharmacia Biotech, Arlington Heights, IL) for 2 hr. Blots were washed extensively, air-dried, and exposed to PhosphorImager screens (Molecular Dynamics, Sunnyvale, CA) for 2–4 d.

After quantitation of bound radioactivity with the ImageQuant software package on a Molecular Dynamics PhosphorImager, analysis was performed as follows. Tubulin immunoreactivity in one mouse type was divided by that in wild-type mice to obtain a value that was then compared statistically with 1.0 using Data Desk software. Because equal amounts of starting MT fractions were loaded for each mouse type, mice with the same amount of total tubulin in the MT fraction should give a value of 1.0. Significant increases or decreases in tubulin levels would give values significantly different from 1.0. Ratios of MAP to tubulin were similarly compared between mouse types. Three or four mice of each type were used, and the results were averaged.

Electron microscopy and morphometry of mouse optic nerve. For analysis of microtubule number and density, anesthetized mice were sacrificed, and optic nerves were immediately removed, cut into 1–2 mm segments, and placed into fixative containing 2% paraformaldehyde, 2% glutaraldehyde in freshly made cacodylate buffer, pH 7.2, at 37°C (de Waegh et al., 1992). After 2–3 hr of initial fixation, the nerves were placed in fresh fixative overnight at 4°C. The next day, the nerves were osmicated, dehydrated, and embedded in Epon. Thin sections were counterstained with uranyl acetate and lead citrate and viewed with a JEOL 1200SX electron microscope. Axons cut in cross section were photographed at 50,000×.

MT densities were quantitatively evaluated in shiverer, MBP/MBP transgenic, and wild-type mouse optic nerve axons by overlaying a transparency of evenly spaced hexagons onto electron micrographs printed at a final magnification of 140,000× (Price et al., 1988). At this magnification, each hexagon represented 0.035 μm^2 of axoplasm. The number of MTs present in each hexagon was counted. Hexagons that were not >90% within the axonal boundaries and axons for which membrane-bounded organelles occupied >10% of the cross-sectional area, or in which the MTs were cut tangentially, were excluded from analysis. At least 60 axons (370 hexagons) were counted for each mouse type. The cross-sectional area of each axon counted was estimated by measuring the diameter at several points, then calculating the area of the best fit ellipse. Additionally, the number of myelin wraps was noted for each axon counted. The average number of MTs per hexagon was calculated by dividing the total number of MTs counted by the total number of hexagons. Significant differences were determined by a two-sample, two-sided *t* test using Data Desk software.

For analysis of axon caliber, optic nerve sections were obtained as described previously (Shine et al., 1992). Briefly, mice were anesthetized with Avertin, then perfused intracardially with 1% paraformaldehyde and 2.5% glutaraldehyde in 0.1 M phosphate buffer, pH 7.4. After perfusion, the optic nerves were dissected, fixed overnight in the same fixative at 4°C, washed in phosphate buffer with 5% sucrose, and post-fixed with 2% OsO_4. Nerves were then processed for Epon embedding. Sections were counterstained with uranyl acetate and lead citrate, and micrographs were taken at 8000× magnification. Each negative was printed to give a 30,000× magnification, and axons were numbered and categorized as unmyelinated (no compact myelin encircling the axon), myelinated, or wrapped. An axon was considered wrapped if surrounded by one or more layers of oligodendrocyte uncompacted membrane. Only axons that were cut perpendicular to their long axis were included in the analysis. Circumference and axonal area were measured by manually tracing axon perimeters directly from the photographs on a digitizing tablet. The values were computed with Sigma Scan morphometric software (Jandel Scientific, Corte Madera, CA) that was calibrated against an

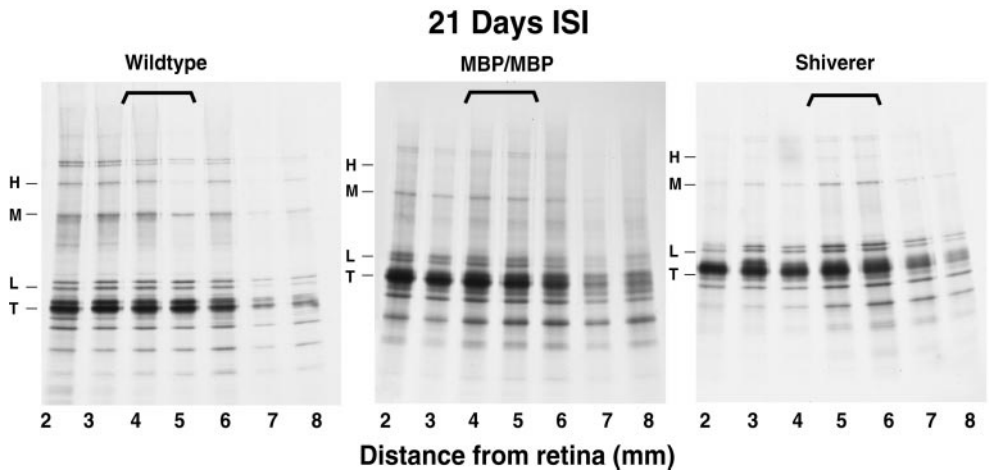

Figure 1. Axonal transport of tubulins in shiverer, transgenic, and wild-type mouse optic nerve. Slow axonal transport rates were examined by segmental analysis. ^{35}S-methionine was injected into the vitreous of the mouse eye, and 21 d after injection, optic nerve–optic tracts were harvested and cut into 1 mm segments. Radioactively labeled proteins in each segment were resolved on SDS-PAGE gels, processed for fluorography, and exposed to film. Fluorographs of wild-type, MBP/MBP transgenic, and shiverer optic nerve show a wave of radioactively labeled SCa proteins traveling down the optic nerve–optic tract. Radiolabeled tubulin (*T*) and the neurofilament triplet subunits (H, M, and L) are distributed as a wave along the nerve in all three animals at 21 d after injection, but the position of the peak differs. The peak for tubulins is in axon segments 4–5 mm for wild-type and MBP/MBP nerves but in segments 5–6 mm for shiverer. Note that the fraction of SCa-labeled proteins in the tubulin band is higher in shiverer and MBP/MBP nerves than in wild type.

electron micrograph of a grating replica (Ted Pella, Redding, CA) at the same magnification.

Determination of tubulin mRNA levels. Oligonucleotide probes were designed against regions conserved in all α-tubulins or all β-tubulins (ACC ATC TGG TTG GCT GGC TCA AAG CAG GCA TTG GTG ATC TCT GC and GAG ATG CGC TTG AAC AGC TCC TGG ATG GC, respectively). In addition, oligonucleotide probes were designed against the housekeeping enzyme glyceraldehyde-3-phosphate dehydrogenase (GAPDH) to wild type for loading (CAG GGG GGC TAA GCA GTT GGT GGT GCA GGA TGC ATT GCT G). Probes were end-labeled in a reaction catalyzed by the T4 polynucleotide kinase enzyme (Life Technologies, Gaithersburg, MD), and unincorporated nucleotides were removed by filtration through a G-50 column (Amersham Pharmacia Biotech, Piscataway, NJ). An aliquot of the reaction was used to measure incorporation, and the specific activity of the probe was calculated (typically between 1 and 2.5×10^9 cpm/μg).

Brain RNA was extracted from wild-type, transgenic, and shiverer mice using the method of Chomzynski and Sacchi (1987). Total RNA (5 μg) was electrophoresed on a 1% denaturing agarose gel, transferred to a nylon membrane (Nytran; Schleicher & Schuell, Keene, NH), and UV cross-linked using a Bio-Rad UV Irradiator (Bio-Rad, Hercules, CA). The membrane was stained with a methylene blue solution to assess transfer and loading. After the membrane was incubated for 2 hr in prehybridizing solution containing 6× SSPE, 6× Denhardt's solution, 0.5% SDS, and 0.2 μg/ml sheared herring sperm DNA, oligonucleotide probes were added to a final concentration of 2×10^6 cpm/ml. Probes were hybridized overnight, and blots were washed to a final stringency of 2× SSC, 2% SDS at 37°C. Membranes were exposed to a PhosphorImager screen (Kodak Eastman, Rochester, NY), and the resulting signals were digitized using a PhosphorImager (Molecular Dynamics). For each probe, signals were expressed as a ratio of the experimental probe to the housekeeping enzyme GAPDH (Tso et al., 1985) to standardize the experimental mRNA levels to a specific amount of starting material. Levels of GAPDH are reported not to vary in shiverer and transgenic animals relative to wild type, allowing a groupwise comparison of experimental RNA levels between animals.

RESULTS

Slow axonal transport

Slow axonal transport rates are differentially affected in PNS neurons of the dysmyelinating mutant Trembler mouse. Transport of the NF proteins and most SCb proteins is slower in Trembler, whereas mean tubulin transport occurs at a faster rate (de Waegh and Brady, 1990). To determine whether similar changes occur in poorly myelinated CNS axons, slow axonal transport rates were measured in shiverer, transgenic, and wild-type B6C3/F1 mouse optic nerve axons using the segmental analysis method (Brady, 1985). Intraocular injection of ^{35}S-methionine was used to label newly synthesized proteins in retinal ganglion cell neurons, and axonal proteins were subsequently analyzed in the optic nerve–optic tract after ISIs appropriate for SCa (18–24 d) or SCb (4–5 d). Tubulin and NFM were used as marker proteins for SCa, whereas clathrin, actin, and spectrin were used to follow SCb.

Table 1. Slow axonal transport rates in shiverer, MBP/MBP transgenic, and wild-type mouse optic nerve: movement of the 50% point, rates in millimeters per day

SCa	Tubulin	NFM
Shiverer ($n = 5$)	0.22 ± 0.03^a	0.20 ± 0.02^b
MBP/MBP ($n = 8$)	0.16 ± 0.04	0.17 ± 0.03
Wild type ($n = 6$)	0.18 ± 0.03	0.17 ± 0.03
SCb	Clathrin	Spectrin
Shiverer ($n = 4$)	0.93 ± 0.08^c	0.96 ± 0.08^d
MBP/MBP ($n = 6$)	0.74 ± 0.10	0.74 ± 0.11
Wild type ($n = 7$)	0.83 ± 0.16	0.82 ± 0.12

[a]Shiverer tubulin significantly different from MBP/MBP, $p = 0.01$; and wild type, $p = 0.05$.

[b]Shiverer NFM significantly different from MBP/MBP, $p = 0.03$; and wild type, $p = 0.05$.

[c]Shiverer clathrin significantly different from MBP/MBP, $p = 0.02$.

[d]Shiverer spectrin significantly different from MBP/MBP, $p = 0.008$; and wild type, $p = 0.03$.

Initial observation of the fluorographs from such experiments suggested that SCa transport in the shiverer occurs at a faster rate (Fig. 1). For example, the tubulins in the shiverer fluorograph appear to peak in segments 2–5, whereas in wild-type mouse fluorographs, and also in transgenic, the tubulins are still primarily in segments 1–3. Quantitation of the incorporated radioactivity in each protein band facilitated the determination of axonal transport rates, which are summarized in Table 1. Both SCa and SCb proteins move at a faster rate in shiverer optic nerve axons. SCa-carried tubulin and NFM move at a rate of 0.2–0.22 mm/d in shiverer axons but at 0.16–0.18 mm/d in wild-type and transgenic axons. SCb-carried spectrin, clathrin, and actin move at a rate of 0.93–0.96 mm/d in shiverer but at 0.74–0.86 mm/d in wild type and transgenic. These rate increases are significantly different from wild type and indicate that CNS myelination affects slow axonal transport of cytoskeletal proteins. However, unlike PNS demyelination, which results in a decreased transport rate for

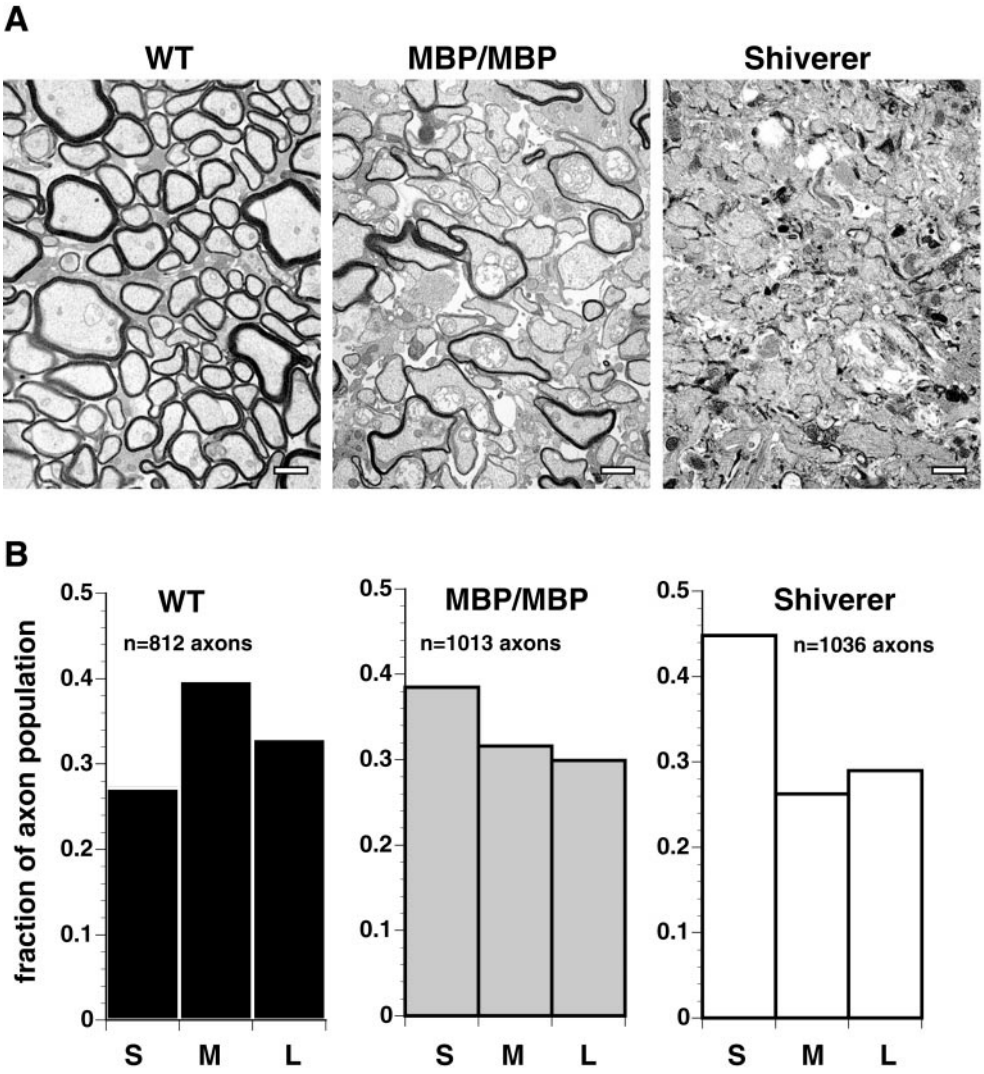

Figure 2. Distribution of axonal calibers is affected by myelination. *A*, Electron micrographs of optic nerve from wild-type (*WT*), transgenic (*MBP/MBP*), and shiverer (*Shiverer*) mice exhibit striking differences in myelination. No compact myelin is apparent in shiverer nerves, and compact myelin in MBP/MBP nerve is much reduced relative to wild type. *B*, Morphometric analysis of axon caliber in optic nerve from wild-type and mutant mice shows a shift in axon caliber with increasing levels of compact myelin. Optic nerve axons are among the smallest myelinated axons and are relatively uniform in size. However, 45% of the axons in shiverer nerve have an area of <0.2 mm^2 [small (*S*)], in contrast to wild-type nerve in which only 27% fell into the *S* category. Most axons in wild-type nerve were in the medium (*M*; 40%) or large (*L*; 33%) categories, whereas in shiverer there were 26% in the *M* and 28% in the *L* categories. In MBP/MBP nerves, the axon area phenotype was intermediate, consistent with an intermediate level of compact myelin. As with shiverer nerve, the largest number of axons were categorized as *S*, but the fraction in *S* was only 38%, with 32% in *M* and 30% in *L*.

most proteins (de Waegh and Brady, 1990), lack of CNS myelin results in faster transport rates of cytoskeletal proteins. Interestingly, transport rates were not significantly different between transgenic and wild-type mice, indicating that even a partial restoration of normal compact myelin levels is sufficient for normal slow axonal transport rates.

Electron microscopy and morphometry

To determine whether lack of CNS myelin affected cytoskeletal organization in shiverer axons in a manner comparable with that seen with PNS demyelination, wild-type, shiverer, and transgenic mouse optic axons were analyzed by electron microscopy (EM). Although others have looked at shiverer and transgenic axons by EM (Shine et al., 1992), previous analyses focused on the myelin, and little information was provided on the composition or organization of cytoskeletal elements inside the axon. A striking change in cytoskeletal density was observed even at low magnification in both shiverer and transgenic optic nerve axons (Fig. 2). Because it was apparent at higher magnification that the major contributor to the increased density was MTs, a detailed morphometric analysis of MT density was performed. MT densities were counted in cross sections of shiverer, transgenic, and wild-type optic nerve axons by overlaying a transparent sheet of evenly spaced hexagons onto electron micrographs. At least 60 axons of different sizes were examined in each animal type, corresponding to >370 hexagons and >13 μm^2 of axonal area. Table 2 summarizes the total number of axons and hexagons counted and the mean MT density for each of the three mouse types.

When the total number of MTs counted is divided by the total number of hexagons counted, the average number of MTs per hexagon is obtained. Supporting the initial EM observations, there is a significant twofold increase in the density of MTs in shiverer and transgenic optic nerve axons ($p \leq 0.0001$, two-sample *t* test). The average number of MTs per hexagon increases from approximately two in the wild type to more than four in the mutant mice. This represents a density of ~125–130 MTs/μm^2 in shiverer and transgenic axons, as compared with only 54 MTs/μm^2 in wild-type axons.

Axons were chosen for this analysis strictly on the basis of whether they were cut in cross section. However, when axons were binned by size, more of the axons counted in shiverer and transgenic optic nerve were small (<0.2 μm^2), whereas most axons counted in wild-type optic nerve were medium (0.2–0.4 μm^2) or large (>0.4 μm^2) in size (Table 2). To examine this question further, large numbers of axons for each mouse type were photographed at low magnification, and axon areas were measured using a computer workstation and morphometric software. The

Table 2. Summary of MT density statistics

	Shiverer	MBP/MBP	Wild type
Total number of axons counted	92	90	64
Small[a]	47	45	20
Medium[a]	34	23	24
Large[a]	11	22	20
Total number of hexagons counted	415	428	373
Area axoplasm counted (μm^2)[b]	14.5	15.0	13.1
Total number of MTs counted	1879	1869	705
MTs/μm^2	129.6	124.6	53.8
Average number of MTs per hexagon (all axons)	4.5[c]	4.4[c]	1.9
Small[a]	6.0[c,d]	6.1[c,d]	3.3[d]
Medium[a]	4.4[c]	4.2[c]	2.2
Large[a]	3.3[c]	3.5[c]	1.3

[a]Small, <0.2 μm^2; medium, 0.2–0.4 μm^2; large, >0.4 μm^2.

[b]Number of hexagons × 0.035 μm^2.

[c]Significantly different from wild type, $p \leq 0.0001$.

[d]Small versus medium, small versus large, and medium versus large significantly different, $p \leq 0.01$-0.0001.

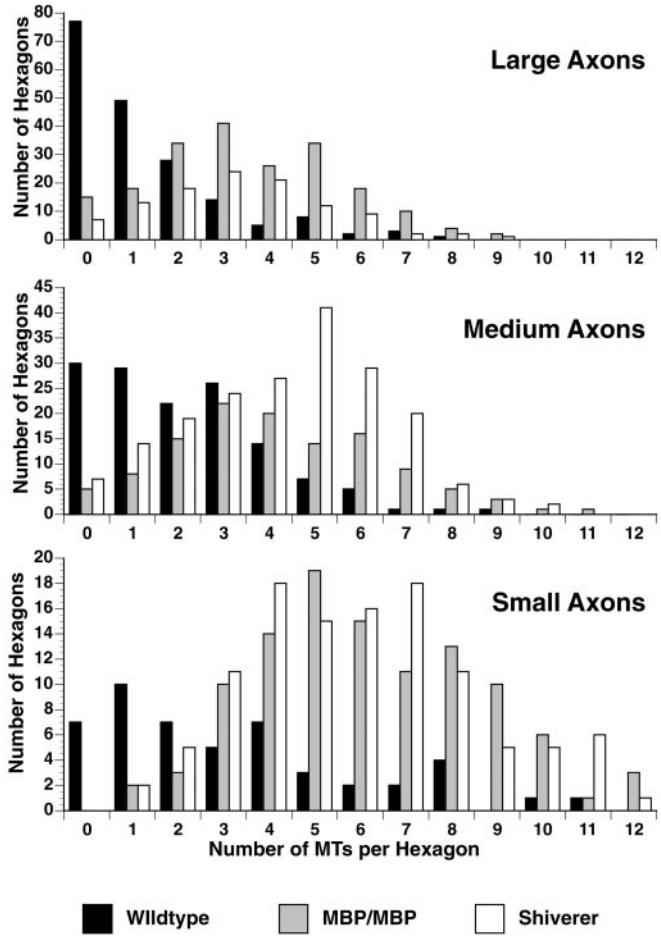

Figure 3. Morphometric analysis of MT distribution shows different densities in different caliber axons. The density of microtubules in wild type, MBP/MBP, and shiverer for different sized axons was analyzed as described previously (de Waegh et al., 1992) by determining the number of cytoskeletal elements in random hexagons. Size categories are as described in Figure 2 and Table 2. Morphometric analyses were conducted by overlaying a hexagonal grid over electron micrographs of the optic axonal cross sections printed at a final magnification of 140,000×. Each hexagon represented an area of 0.035 μm^2. The number of microtubules per hexagon was scored, binned, and plotted. Microtubule densities are shifted to higher values in both shiverer and MBP/MBP axons for all sizes of axon, but the density was greatest in small axons (means of 6.0–6.1 per hexagon in shiverer and MBP/MBP; mean of 3.3 per hexagon in wild type) and correspondingly reduced in medium (4.2–4.4 vs 2.2 per hexagon) and large (3.3–3.5 vs 1.3 per hexagon) axons (Table 2). In all cases, the shiverer and MBP/MBP axons showed similar MT density distributions. These values may be converted to MTs per micrometer^2, giving values for shiverer and MBP/MBP of 170 MTs/μm^2 (S), 123 MTs/μm^2 (M), and 97 MTs/μm^2 (L), as compared with 94 MTs/μm^2 (S), 63 MTs/μm^2 (M), and 37 MTs/μm^2 (L) for wild-type axons.

results presented in Figure 2*B* indicate that there is a higher percentage of small axons in shiverer and transgenic optic nerves.

To ensure that the average number of MTs per hexagon calculated was not biased by the preponderance of one axon size in a given mouse type and to determine whether MT densities varied with axon size, MT densities were calculated individually for each axon size category (Fig. 3). The average number of MTs per hexagon in shiverer and transgenic optic nerve was approximately twice that found in wild-type nerve for all axon sizes, and in every case the difference was significant (Table 2) ($p \leq 0.0001$, two-sample *t* test). For example, in small axons, the average number of MTs per hexagon in shiverer and transgenic was 6.0–6.1, whereas in wild-type nerves there were only 3.3 MTs per hexagon. Similarly, shiverer and transgenic mice averaged 3.3–3.5 MTs per hexagon in large optic axons, but MT densities were only 1.3 in comparably sized wild-type axons.

Interestingly, changes in the number of MTs per hexagon from small to medium to large axons were significant as well (Fig. 3, Table 2). For example, in wild-type axons, the average number of MTs per hexagon shifts from 3.3 in small axons to 1.3 in large axons, a significant decrease ($p \leq 0.0001$, two-sample *t* test). In contrast, the shift in MT density in shiverer axons was from 6.0 in small axons to 3.3 in large axons ($p \leq 0.0001$, two-sample *t* test). This result was consistent with previous observations that the NF number correlates best with axon size for large axons >1 μm in diameter, but that the MT number correlates best with axon size for fibers <1 μm in diameter (Friede and Samorajski, 1970). As noted here, most optic axons in mouse are <1 μm in diameter. These data demonstrate that deficiencies in CNS myelin result in a twofold increase for MT density in shiverer and transgenic axons, but MT density still decreases as axon size increases. This indicates that some regulation of axonal MT density is still present even in the absence of myelin.

To determine whether MT density correlates with myelin thickness even in mice lacking normal levels of compact myelin, we plotted the average number of MTs per hexagon versus the increasing number of myelin wraps. Because myelin thickness is correlated with axon size (Friede and Miyagishi, 1972), these calculations were done with all axons and not for small, medium, and large separately (Table 3). In wild-type mouse axons with four to five myelin wraps (the lowest level of myelin found on wild-type axons), the average number of MTs per hexagon was 2.5. This value drops to 1.5 MTs per hexagon in axons with 11 or more myelin wraps, a significant decrease ($p \leq 0.0001$, two-sample *t* test). Similarly, the average number of MTs per hexagon in transgenic axons with no myelin (5.5 MTs) or 1 myelin wrap (4.8 MTs) drops significantly to 2.9 in axons with 6–10 myelin

Table 3. Average number of MTs per hexagon decreases with increasing myelin thickness

Number of myelin wraps	Shiverer[a]	MBP/MBP	Wild type
0	5.1[b]	5.5[c]	
1	4.5	4.8	
2–3	4.4	4.6	
4–5		3.9[d]	2.5[e]
6–10		2.9[d]	2.3
11+			1.5

[a]No shiverer axons were found with compact myelin, but in some cases an oligodendrocyte process was seen to wrap the axon two or three times.

[b]Shiverer: 0 wraps significantly different from 2–3 wraps, $p \leq 0.01$.

[c]MBP/MBP: 0 wraps significantly different from 4–5 wraps, $p \leq 0.007$; 0 wraps significantly different from 6–10 wraps, $p \leq 0.0001$.

[d]Significantly different from wild type, $p \leq 0.01$-0.001.

[e]Wild type: 4–5 wraps significantly different from 11+ wraps, $p \leq 0.0001$.

wraps. In shiverer optic nerve, unmyelinated axons have an average of 5.1 MTs per hexagon, whereas axons with two to three wraps of myelin have an average of 4.4, a difference that was significant at $p \leq 0.01$ (two-sample t test). However, in both shiverer and transgenic optic nerves, the mere wrapping of an axon by an oligodendrocyte was not enough to cause a significant decrease in MT density. Significant decreases were not seen in transgenic axons until four to five wraps were present or in shiverer axons with fewer than two to three wraps.

To summarize, these morphometric studies demonstrate a significant twofold increase in MT density in shiverer and transgenic optic nerve axons as a result of deficient CNS myelination. This increased MT density was apparent in all axon sizes and at all levels of myelination. However, these axons did show decreases in MT density that correlated with increases in axon size and myelination. This variation suggests that there must be multiple, distinct signals from myelinating glia that regulate different aspects of the axonal MT cytoskeleton.

Quantitation of MT protein

Because morphometric analysis indicated that microtubule numbers were increased in shiverer and transgenic axons, levels of brain tubulin and microtubule-associated proteins were evaluated in two ways. First, the amount of tubulin labeled by slow axonal transport was determined. As described previously for neurofilament proteins (Brady et al., 1999), the amount of radioactivity incorporated into an axonal protein may be quantitated by excising bands from gels using fluorographs as a template. To normalize for labeling efficiency, amounts need to be expressed as a fraction of total labeled proteins in SCa.

In these studies, optic nerves containing labeled SCa proteins were fractionated to evaluate the stability of the axonal microtubules in wild-type, shiverer, and transgenic axons (see below) using SDS-PAGE and fluorography as described previously (Brady et al., 1984; Kirkpatrick and Brady, 1994). The amounts of total labeled SCa protein and axonal tubulin were measured by excising all radiolabeled bands and spaces between them from the gels and measuring the amount of radioactivity recovered in each gel slice. The sum of radioactivity recovered in all fractions was determined, and this total was used to standardize relative levels of specific polypeptides as a percentage of total SCa protein. The percentage of total SCa radioactivity associated with the tubulin was then calculated (Fig. 4). The amount of tubulin in SCa was significantly

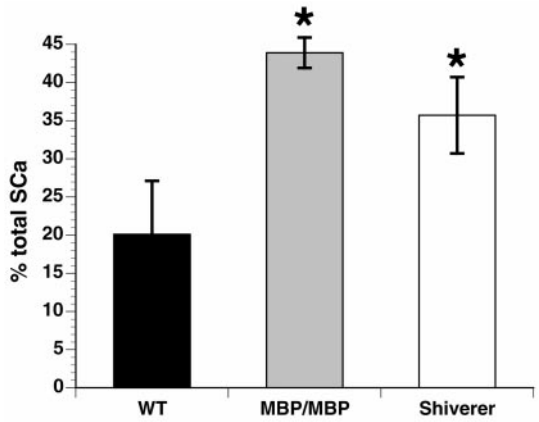

Figure 4. Tubulin levels may be quantitated from axonal transport studies. Differences in the amount of tubulin in optic axons may be seen by measuring the total amount of labeled tubulin in the nerve at a given time point and expressing it as a ratio of the total amount of labeled protein in the nerve at the same time. Tubulin represented 20% of labeled protein in wild-type axons, but was 44% of labeled protein in MBP/MBP axons and 36% in shiverer axons. This indicates that the amount of tubulin committed to slow axonal transport is increased in the absence of a normal complement of compact myelin. *Asterisk* indicates significant difference when compared with wild-type ($p \leq 0.02$).

increased relative to wild-type optic nerves for both shiverer and transgenic nerves. Approximately 35% of total SCa radioactivity was associated with tubulin in shiverer, and >40% was tubulin in transgenic. In contrast, only 20% of total SCa radioactivity corresponded to tubulin in wild-type optic nerves. This increase was significant ($p \leq 0.02$, two-sample t test), indicating that tubulin protein levels were increased in shiverer and transgenic.

These observations were extended by quantitative immunoblot analysis. Whole-brain MTs were prepared from each mouse type, and equal amounts of total protein were analyzed by immunoblotting with antibodies directed against tubulin and MAPs (Fig. 5*A*). There was a significant increase in the amount of tubulin in brain MT fractions prepared from shiverer and transgenic when compared with wild type ($p \leq 0.01$, two-sample t test). This result is in agreement with that obtained above and further supports the possibility that tubulin expression is increased in axons without myelin. As noted previously for NF protein levels (Brady et al., 1999), both shiverer and transgenic tubulin levels differ from wild-type tubulin levels, indicating that the presence of a thinner than normal compact myelin sheath is not sufficient to regulate tubulin levels normally. Associated proteins are critical for normal MT function in neurons, so it was of interest to determine whether MAP levels are also altered in these mice. Antibodies directed against the high molecular weight MAPs 1A and 1B and tau were used on immunoblots of equal amounts of shiverer, transgenic, and wild-type mouse brain MT fractions. Changes in both the level and composition of these MAPs were seen in shiverer and transgenics as well (A. S. Witt and S. T. Brady, unpublished observations).

Quantitation of tubulin mRNA expression

Increases in tubulin protein levels could be attributed to increases in tubulin synthesis, increases in tubulin stability, or decreases in tubulin turnover. To determine whether tubulin synthesis was altered, levels of steady-state tubulin mRNA were evaluated by Northern analysis. Total brain RNA from the different animals was hybridized to radiolabeled probes directed against regions

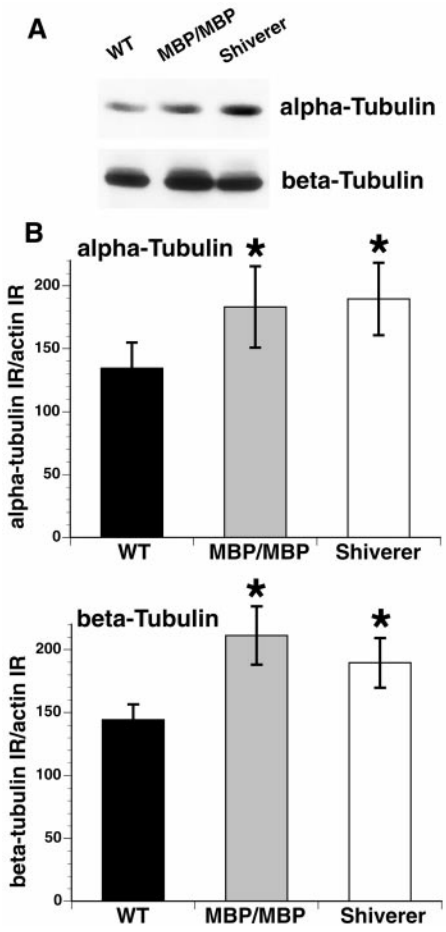

Figure 5. Total brain tubulin is increased relative to total brain actin in shiverer and MBP/MBP mice. *A*, Quantitative immunoblots using antibodies specific for α- and β-tubulin show that total brain tubulin immunoreactivity is increased in both shiverer and MBP/MBP mice. *B*, Normalization of tubulin immunoreactivity to actin immunoreactivity in the same samples allows a quantitative comparison of changes in tubulin immunoreactivity in brain. Brain α-tubulin immunoreactivity is increased by 36% in MBP/MBP brain and by 41% in shiverer brain relative to that seen in wild-type brains. Similarly, brain β-tubulin immunoreactivity is increased by 46% in MBP/MBP brain and by 31% in shiverer brain relative to that seen in wild-type brains. *Asterisk* indicates significant difference when compared with wild-type ($p \leq 0.01$).

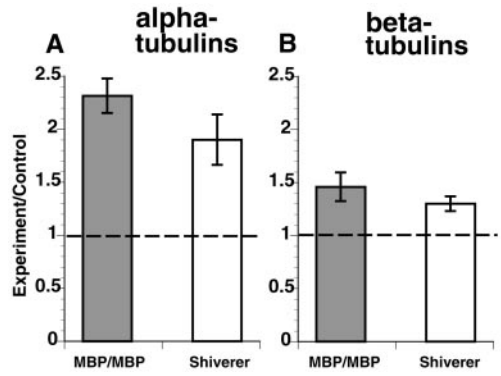

Figure 6. Quantitative Northern blots indicate that tubulin mRNA levels are increased in shiverer and MBP/MBP mouse brains. RNA fractions from retina were probed with oligonucleotides shared with all known mouse α- or β-tubulins as well as one for GAPDH as a loading control. After correction for mRNA load with GAPDH, a ratio of mutant to wild-type expression levels for both α- and β-tubulin was calculated. The levels of both α- and β-tubulin mRNA expression were significantly increased for shiverer and MBP/MBP relative to wild type. As with changes in tubulin protein levels, α- and β-tubulin RNA levels were significantly increased in MBP/MBP and shiverer mice relative to wild type ($p = 0.0002$ and 0.009 for α-tubulin, $p = 0.02$ and 0.007 for β-tubulin, in transgenic and shiverer, respectively).

conserved in all α-tubulins ("pan α-tubulin") (Fig. 6*A*) and all β-tubulins ("pan β-tubulin") (Fig. 6*B*). The signal levels were corrected for loading using signals against the housekeeping enzyme GAPDH, normalized to wild-type levels, and plotted ($n = 11$ experiments using RNA from seven animals in each category). As with tubulin protein levels, α- and β-tubulin RNA levels are significantly increased in transgenic and shiverer animals relative to wild type ($p = 0.0002$ and 0.009 for α-tubulin, $p = 0.02$ and 0.007 for β-tubulin, in transgenic and shiverer, respectively). Significance was determined by two-sample *t* test.

Cold-calcium fractionation of axonal MTs

The stability of axonal MTs in sciatic nerves of the PNS demyelinating mutant Trembler is dramatically reduced, as measured by a biochemical cold-calcium fractionation assay using radiolabeled SCa-carried MTs (Kirkpatrick and Brady, 1994). To determine whether CNS myelination also affects MT stability, the cold-calcium fractionation was performed on SCa-carried MTs in shiverer, transgenic, and wild-type mouse optic nerve axons. This two-step extraction protocol is based on standard procedures for the preparation of MTs from whole brain and results in three fractions: S1, which contains cold-soluble proteins; S2, which contains cold-insoluble, but calcium-soluble proteins; and P2, which contains cold- and calcium-insoluble proteins (Brady et al., 1984). Typically, when adult rodent axonal MTs are fractionated, >50% partition into the cold-calcium-insoluble P2 fraction.

Optic axon MTs in SCa were labeled by injection of ^{35}S-methionine into the vitreous of the mouse eye. The entire optic nerve–optic tract was removed and fractionated by the cold-calcium protocol 24 d after labeling. Resulting S1, S2, and P2 fractions were analyzed by SDS-PAGE and fluorography. The radioactivity present in tubulin and NF protein bands was quantitated; the values for S1, S2, and P2 were added, and each was expressed as a percentage of the total (Table 4, Fig. 7).

In wild-type mouse optic nerve, 38% of SCa-labeled MTs were cold-soluble and 55% were cold-insoluble. These values are consistent with those obtained in the Trembler studies (Kirkpatrick and Brady, 1994) and in previous studies in rat (Brady et al., 1984). In contrast, >66% of SCa-labeled MTs were cold soluble, and only 27% were cold insoluble in shiverer optic nerves, a significant decrease in MT stability ($p \leq 0.005$, by a two-sample *t* test). Similarly, transgenic optic nerve contains only 27% stable MTs, also a significant decrease from wild type. In both shiverer and transgenic mice, the level of tubulin is significantly increased, but two-thirds of the tubulin in their axons is associated with labile, potentially dynamic MTs. Both of these characteristics are typically associated with nerve fibers in the developing nervous system (Brady and Black, 1986). However, not all aspects of the MT cytoskeleton in shiverer and transgenic are equivalent. Because slow axonal transport rates for tubulin in the transgenic mice were comparable with wild-type rates, this indicates that increases in cold-stable tubulin levels are not a direct determinant of tubulin axonal transport rates. Furthermore, the mere presence of compact myelin is not enough to generate normal levels of stable MTs.

Table 4. Cold-calcium fractionation of SCa-labeled tubulin and NF proteins

	S1	S2	P2
Tubulin			
Shiverer	66.5 ± 8.7	5.9 ± 1.7	27.5 ± 9.1[a]
MBP/MBP	69.8 ± 1.6	3.1 ± 1.3	27.0 ± 1.2[a]
Wild type	38.0 ± 4.0	7.1 ± 2.0	54.9 ± 4.0
NFL			
Shiverer	34.8 ± 9.6	6.2 ± 1.8	59.0 ± 9.0
MBP/MBP	36.9 ± 5.7	4.7 ± 1.3	58.5 ± 6.0
Wild type	26.5 ± 12.0	6.5 ± 4.2	67.1 ± 15.0
NFM			
Shiverer	47.4 ± 18.7	6.6 ± 3.2	46.0 ± 17.0[b]
MBP/MBP	21.5 ± 8.0	2.7 ± 0.7	77.5 ± 10.5
Wild type	25.4 ± 11.5	10.3 ± 6.0	70.4 ± 16.5
NFH			
Shiverer	33.2 ± 4.8	8.5 ± 4.2	58.4 ± 5.5
MBP/MBP	22.4 ± 13.1	5.0 ± 2.2	73.7 ± 16.0
Wild type	21.2 ± 10.1	7.4 ± 7.1	73.5 ± 19.0

[a] Significantly different from wild type, $p \leq 0.005$.
[b] Significantly different from MBP/MBP, $p \leq 0.03$.

Unexpectedly, cold-calcium fractionation of SCa proteins was also informative about properties of axonal NFs in wild-type, transgenic, and mutant mice. Typically, >70% of NF proteins are associated with P2 fractions in cold-calcium fractionations (Brady et al., 1984), consistent with the high degree of stability of neuronal intermediate filaments. As expected, >70% of NF protein was in P2 for both wild-type and transgenic optic nerve (Table 4, Fig. 7). However, the amount of NF protein in P2 fraction was significantly reduced in shiverer nerves. The fraction of NFM in P2 fractions of shiverer nerves was <50%, significantly less than seen for either transgenic or wild type ($p \leq 0.02$, by two-sample *t* test). The amount of NFH in P2 fractions of shiverer nerve was similarly reduced.

These results suggest that the absence of CNS myelin affects the stability of the NF cytoskeleton as well as the MT cytoskeleton. As noted previously, one difference between the shiverer and wild-type axonal cytoskeleton is that shiverer NFs have reduced the stoichiometry of NFH and NFM to NFL (Brady et al., 1999). In contrast to shiverer, transgenic axons contained NFs with a normal stability. As in shiverer mice, NFs in transgenic axons were deficient in NFH, but, unlike in shiverer, transgenic NFs contained normal levels of NFM. This compositional difference provides a likely explanation for differences in NF stability. It would appear that increased levels of NFM are necessary and sufficient for increasing the stability of axonal NFs.

The fact that NFs in transgenic nerves exhibited wild-type stability but MTs in transgenic nerves remained labile indicates first that the mechanisms regulating stability of these cytoskeletal elements are different, and second that NF and MT stability are not directly linked to one another. Furthermore, there must be multiple regulatory signals conveyed by the myelinating glia. In summary, morphometric, immunochemical, and cold-calcium fractionation analyses of wild-type, shiverer, and transgenic optic nerve indicate that myelination affects both the stability and the composition of the MT cytoskeleton in the CNS.

DISCUSSION

The environment established by myelinating glia affects a wide range of neuronal properties, including composition, organization, and transport of the axonal cytoskeleton. In Trembler, disruption of normal PNS axon–glia relationships alters slow axonal transport rates, MT stability, NF phosphorylation, and cytoskeletal organization (de Waegh and Brady, 1990, 1991; de Waegh et al., 1992; Kirkpatrick and Brady, 1994). Myelination by Schwann cells primarily affected local axonal properties. However, axonal microtubule composition was also changed (Kirkpatrick and Brady, 1994). The effects of Schwann cells on PNS axonal MTs implied that CNS axonal MTs might also be modulated by myelination.

CNS oligodendrocyte myelin differs from PNS Schwann cell myelin in developmental origin and composition. Such differences presumably have functional consequences. For example, PNS

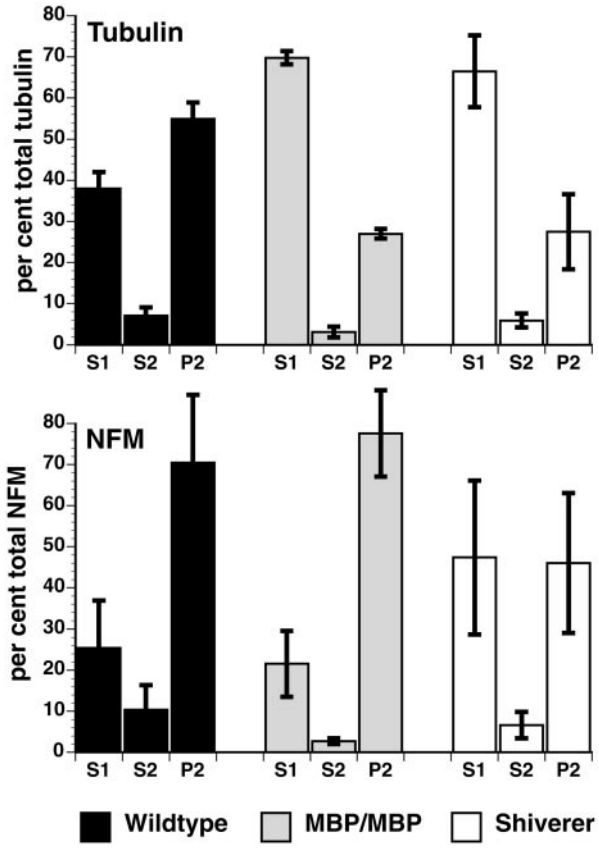

Figure 7. Cold-calcium fractionation of SCa-labeled cytoskeletal proteins indicates that myelination affects the stability of the axonal cytoskeleton. Using our standard cold-calcium fractionation protocols (Kirkpatrick and Brady, 1994), the stability of the microtubule and neurofilament cytoskeletons may be analyzed. As in Trembler peripheral nerve, the amount of tubulin in the P2 fraction (*top panel*) is substantially reduced in the absence of myelin (shiverer). As with other parameters associated with the axonal microtubule cytoskeleton, the thin myelin sheath in MBP/MBP optic axons is not sufficient to increase the amount of cold-calcium-insoluble tubulin in P2 (*top panel*). In both mutant mice, cold-calcium-insoluble tubulin fractions are reduced by half, and extractable tubulin is correspondingly increased. Unlike Trembler peripheral nerve, however, a difference in the stability of the neurofilament cytoskeleton was also observed (*bottom panel*). When compact myelin was completely absent (shiverer), the amount of NFM found in the stable fraction dropped from 71 to 47% with a corresponding increase in the extractable form. However, even a thin myelin sheath was sufficient to reverse this effect, because MBP/MBP values are comparable with wild type. Similar changes in neurofilament stability were seen for NFL and NFH as well (Table 4). These data suggest that myelination leads to stabilization of both microtubule and neurofilament axonal cytoskeletons, but the effects on microtubules and neurofilaments are modulated independently.

neurons typically regenerate axons efficiently, but CNS neurons do not. The reasons for this discrepancy are poorly understood, but they include the differential effects of glia on axons, because CNS neurons grow well in grafts containing PNS glia (Richardson et al., 1980; Aguayo et al., 1981; Benley and Aguayo, 1982; Vidal-Saenz et al., 1987), and CNS glial surface molecules inhibit neurite outgrowth (for review, see Schwab, 1996). These may result from differential effects of CNS and PNS glial environments on the axonal cytoskeleton, which largely determines axonal growth potential (Brady, 1993).

Studies on Trembler mutant mice defined a paradigm for analyzing the consequences of disrupting axon–myelin interactions (de Waegh et al., 1992). To study axon–oligodendrocyte interactions, shiverer mice were used because they produce no compact CNS myelin (for review, see Readhead and Hood, 1990). The absence of CNS compact myelin produces a severe intention tremor and life-spans of 90–150 d. PNS proteins with overlapping function mean that shiverer PNS compact myelin exhibits only minor structural differences (Gould et al., 1995).

Given that myelin sheath thickness is correlated with axon diameter and adjusts to changes in axon diameter (Friede and Miyagishi, 1972), the availability of transgenic mice expressing an MBP transgene on a shiverer background (Readhead et al., 1987) provides insight into functional linkages between sheath thickness and axonal diameter. Transgenics homozygous for the MBP transgene expressed only 25% of wild-type MBP levels, yielding a thinner compact myelin sheath (Readhead et al., 1987; Shine et al., 1992). The thin myelin sheath produced by limiting amounts of MBP is sufficient to eliminate tremors and restore life-span to wild-type levels (Readhead et al., 1987). Analysis of the axonal cytoskeleton in mice with different myelination levels distinguished between parameters restored by the mere presence of compact myelin and those requiring a full complement of compact myelin.

Slow axonal transport rates for NFs were 15–30% faster in shiverer than wild type (Brady et al., 1999), and comparable shifts were seen in shiverer tubulin transport rates. Rates were near normal in transgenics. Slow transport motors are poorly understood, but increased slow axonal transport rates are a hallmark of developmentally immature axons (Hoffman et al., 1983). Increased slow transport rates in shiverer axons suggest that the formation of compact myelin directly or indirectly reduces slow axonal transport rates during maturation. Even a thin compact myelin sheath restores transport rates to near normal in transgenic axons. Slowed axonal transport was not a function of reduced MT numbers, because MT numbers remain elevated in transgenic axons. Similarly, neither increased phosphorylation nor upregulation of NFH levels is required for reduced slow transport rates, because these are comparable in shiverer and transgenic mice (Brady et al., 1999). A pathway activated by myelination is sufficient to produce this effect. Whether this results from increased NFM levels in transgenics (Brady et al., 1999) or local modulation of transport machinery remains to be determined.

Electron microscopic analysis of shiverer, transgenic, and wild-type optic axons showed that other aspects of shiverer and transgenic axonal cytoskeletons differ dramatically. MT numbers in shiverer and transgenic axons were more than twofold greater than wild-type axons. MT density was increased in shiverer and transgenic axons for all axon sizes and all numbers of myelin wraps, although MT density in transgenics appeared comparable with wild type at the highest number of myelin wraps. Myelin sheath thickness may locally affect axonal MT density, although mechanisms to accomplish this remain uncertain.

Increased MT numbers implied that cytoskeletal protein expression was influenced by myelination. Analysis of SCa determined the fraction of total SCa radioactivity represented by constituent proteins. Such analyses indicated that both shiverer and transgenic axons contained a significantly larger fraction of tubulin. Comparable increases in brain tubulin were seen with quantitative immunoblots. Tubulin levels typically decrease concurrent with increased NFs during neuronal development and maturation, so elevated axonal tubulin was consistent with shiverer and transgenic neurons being immature. The mere presence of compact myelin was not sufficient to reduce tubulin levels, because transgenic tubulin levels remained comparable with shiverer.

Elevations in tubulin protein could be explained by changes in tubulin axonal transport, reduced degradation of axonal tubulin, or increased tubulin gene expression. Decreased tubulin transport rates and a constant rate of synthesis could increase axonal tubulin content, but tubulin slow transport rates were increased in shiverer and comparable with wild type in transgenics, eliminating transport rates as an explanation for increased MT density and number. Similarly, studies on metabolic stability of the axonal cytoskeleton suggest that presynaptic terminals are the primary sites of degradation for cytoskeletal proteins (Paggi and Lasek, 1987), with little or no degradation in axons.

Comparisons of tubulin mRNA levels in shiverer, transgenic, and wild-type brains showed substantial increases in both shiverer and transgenics. Increased tubulin mRNA in shiverer and transgenics implies that altered axonal myelin levels affect transcription in neuronal perikarya. To alter gene expression, signals produced during myelination must be transported back to neuronal cell bodies. Such signals might alter tubulin transcription rates, message stability, or translation rates. There are precedents for myelination affecting transcription in neuron perikarya. For instance, steady-state levels of type II sodium channels are elevated in shiverer, presumably reflecting differences in transcriptional or posttranscriptional events in neuronal perikarya (Noebels et al., 1991). Similarly, axonal tau splice isoforms differ in Trembler and wild-type axons, presumably because of altered RNA splicing in perikarya (Kirkpatrick and Brady, 1994).

CNS myelination affected both the amounts and the biochemistry of axonal MT. In wild-type axons, more than half of the axonal tubulin is resistant to solubilization by standard methods of cold extraction, representing a population of stable axonal MTs (Brady et al., 1984; Brady, 1988). Studies of axonal MTs in Trembler showed that cold-insoluble tubulin fractions were significantly reduced with demyelination (Kirkpatrick and Brady, 1994). In adult wild-type mice, 55% of axonal tubulin is resistant to cold-calcium extraction (Brady et al., 1984), but only 30% of PNS axonal tubulin in Trembler PNS axons was cold-calcium insoluble (Kirkpatrick and Brady, 1994). Shiverer and transgenic axonal MTs exhibited similarly increased cold-calcium solubility. Only 27% of axonal tubulin in shiverer and transgenic optic nerves was cold-calcium insoluble. Formation of a thin compact myelin sheath is insufficient for normal regulation of MT stability.

Reduced levels of cold-calcium-insoluble tubulin in Trembler and shiverer nerves are consistent with an immature axonal cytoskeleton in nonmyelinated axons, because cold-calcium-insoluble levels of axonal tubulin are low in young animals and increase with age (Brady, 1984). However, regulation of MT number and stability must involve discrete pathways, because Trembler has reduced cold-calcium-insoluble tubulin with normal amounts of tubulin (Kirkpatrick and Brady, 1994). Furthermore, slowed axonal transport during development cannot be attribut-

able to changes in either MT number or stability, because transgenics have normal slow axonal transport rates but elevated MT numbers and lower levels of stable MTs.

NF stability also differed among shiverer, transgenic, and wild-type axons. NFs are unusually stable and are normally degraded rather than depolymerized. Typically, >70% of axonal NFs are cold-calcium insoluble, but NFs in cold-insoluble fractions were significantly reduced in shiverer optic nerve. In contrast, transgenic nerves had near normal levels of cold-calcium-insoluble NFs. Apparently, NF stabilization occurs with the formation of a compact myelin sheath, whereas MT stabilization requires a higher level of myelination. NF stability is not dependent on MT stability, and vice versa, but both pathways are influenced by myelination. Increased stability of axonal NFs and slower transport rates in transgenic nerves suggest that increased expression of NFM seen with a thin myelin sheath (Brady et al., 1999) may significantly alter physiological properties of axonal NFs.

In conclusion, glial environments established by oligodendrocytes during myelination have both direct and indirect effects on the neuronal cytoskeleton. Changes are seen in composition, organization, stability, and transport of axonal cytoskeletal structures. Failure to form CNS myelin during development has profound effects on neuronal structure and function, suggesting that glial interactions represent an essential step in neuronal differentiation for neurons with large myelinated axons. Neurons appear sensitive to both the amount of myelination and the type of myelinating glia. Although the importance of glia has long been recognized, glia–neuron relationships appear more extensive and complex than previously recognized. Identification of specific signaling pathways by which myelination influences CNS neurons will be essential for understanding normal development and neuropathologies with altered interactions between oligodendrocytes and axons.

REFERENCES

Aguayo A, David S, Bray G (1981) Influence of the glial environment on the elongation of axons after injury: transplantation studies in adult rodents. J Exp Biol 95:231–240.

Benley M, Aguayo A (1982) Extensive elongation of axons from rat brain into peripheral nerve graft. Nature 296:150–152.

Brady S (1985) Axonal transport methods and applications. In: Neuromethods, general neurochemical techniques (Boulton A, Baker G, eds), pp 419–476. Clifton, NJ: Humana.

Brady ST (1984) Increases in cold-insoluble tubulin during aging. Soc Neurosci Abstr 10:273.

Brady ST (1988) Cytotypic specializations of the neuronal cytoskeleton and cytomatrix: implications for neuronal growth and regeneration. In: Cellular and molecular aspects of neural development and regeneration (Haber B, Gorio A, Vellis JD, Perez-Polo JR, eds), pp 311–322. New York: Springer.

Brady ST (1993) Axonal dynamics and regeneration. In: Neuroregeneration (Gorio A, ed), pp 7–36. New York: Raven.

Brady ST, Black MM (1986) Axonal transport of microtubule proteins: cytotypic variation of tubulin and MAPs in neurons. Ann NY Acad Sci 466:199–217.

Brady ST, Tytell M, Lasek RJ (1984) Axonal tubulin and axonal microtubules: biochemical evidence for cold stability. J Cell Biol 99:1716–1724.

Brady ST, Witt A, Kirkpatrick LL, de Waegh SM, Readhead C, Tu P-H, Lee VM-Y (1999) Formation of compact myelin is required for maturation of the axonal cytoskeleton. J Neurosci 19:7278–7288.

Caceres A, Binder LI, Payne MR, Bender P, Rebhun L, Steward O (1984) Differential subcellular localization of tubulin and microtubule-associated protein MAP2 in brain tissue as revealed by immunocytochemistry with monoclonal hybridoma antibodies. J Neurosci 4:394–410.

Chomczynski P, Sacchi N (1987) Single-step method of RNA isolation by acid guanidinium thiocyanate-phenol-chloroform extraction. Anal Biochem 162:156–159.

de Waegh S, Brady ST (1990) Altered slow axonal transport and regeneration in a myelin-deficient mutant mouse: the Trembler mouse as an *in vivo* model for Schwann cell-axon interactions. J Neurosci 10:1855–1865.

de Waegh SM, Brady ST (1991) Local control of axonal properties: neurofilaments and axonal transport in homologous and heterologous nerve grafts. J Neurosci Res 30:201–212.

de Waegh SM, Lee VM-Y, Brady ST (1992) Local modulation of neurofilament phosphorylation, axonal caliber, and slow axonal transport by myelinating Schwann cells. Cell 68:451–463.

Friede RL, Miyagishi T (1972) Adjustment of the myelin sheath to changes in axonal caliber. Anat Rec 17:1–14.

Friede RL, Samorajski T (1970) Axon caliber related to neurofilaments and microtubules in sciatic nerve fibers of rats and mice. Anat Rec 167:379–388.

Gould RM, Byrd AL, Barbarese E (1995) The number of Schmidt-Lanterman incisures is more than doubled in shiverer PNS myelin sheaths. J Neurocytol 24:85–98.

Hoffman P, Cleveland D (1988) Neurofilament and tubulin gene expression recapitulates the developmental program during axonal regeneration. Induction of a specific β-tubulin isotype. Proc Natl Acad Sci USA 85:4530–4533.

Hoffman PM, Lasek RJ, Griffin JW, Price DL (1983) Slowing of the axonal transport of neurofilament protein during development. J Neurosci 3:1694–1700.

Kirkpatrick LL, Brady ST (1994) Modulation of the axonal microtubule cytoskeleton by myelinating Schwann cells. J Neurosci 14:7440–7450.

Laskey RA, Mills AD (1975) Quantitative film detection of 3H and 14C in polyacrylamide gels by fluorography. Eur J Biochem 563:335–341.

Morell P, Quarles RH (1999) Myelin formation, structure, and biochemistry. In: Basic neurochemistry. Molecular, cellular, and medical aspects, Ed 6 (Siegal GJ, Agranoff BW, Albers RW, Fisher SK, Uhler MD, eds), pp 69–93. Philadelphia: Lippincott-Raven.

Noebels JL, Marcom PK, Jalilian-Tehrani MH (1991) Sodium channel density in hypomyelinated brain increased by myelin basic protein gene deletion. Nature 352:431–434.

Oblinger M, Lasek RJ (1988) Axotomy-induced alterations in the synthesis and transport of neurofilaments and microtubules in dorsal root ganglion cells. J Neurosci 8:1747–1758.

Oblinger MM, Szumlas RA, Wong J, Liuzzi FJ (1989) Changes in cytoskeletal gene expression affect the composition of regenerating axonal sprouts elaborated by dorsal root ganglion neurons *in vivo*. J Neurosci 9:2645–2653.

Paggi P, Lasek RJ (1987) Axonal transport of cytoskeletal proteins in oculomotor axons and their residence times in the axon terminals. J Neurosci 7:2397–2411.

Price R, Paggi P, Lasek R, Katz M (1988) Neurofilaments are spaced randomly in the radial dimension of axons. J Neurocytol 17:55–62.

Readhead C, Hood L (1990) The dysmyelinating mouse mutants shiverer (*shi*) and myelin deficient (*shi*^{mld}). Behav Genet 20:213–234.

Readhead C, Popko B, Takahashi N, Shine HD, Saavedra RA, Sidman RL, Hood L (1987) Expression of a myelin basic protein gene in transgenic shiverer mice: correction of the dysmyelinating phenotype. Cell 48:703–712.

Richardson PM, McGuinness UM, Aguayo AJ (1980) Axons from CNS neurones regenerate into PNS grafts. Nature 284:264–265.

Sahenk Z, Brady ST (1987) Axonal tubulin and axonal microtubules: morphologic evidence for stable regions on axonal microtubules. Cell Motil Cytoskeleton 8:155–164.

Schwab ME (1996) Molecules inhibiting neurite growth: a minireview. Neurochem Res 21:755–761.

Shine HD, Readhead C, Popko B, Hood L, Sidman RL (1992) Morphometric analysis of normal, mutant, and transgenic CNS: correlation of myelin basic protein expression to myelinogenesis. J Neurochem 58:342–349.

Suter U, Welcher AA, Ozcelik T, Snipes GJ, Kosaras B, Francke U, Billings-Gagliardi S, Sidman RL, Shooter EM (1992) Trembler mouse carries a point mutation in a myelin gene. Nature 356:241–243.

Tashiro T, Komiya Y (1991) Changes in organization and axonal transport of cytoskeletal proteins during regeneration. J Neurochem 56:1557–1563.

Tetzlaff W, Bisby MA, Kreutzberg GW (1988) Changes in cytoskeletal proteins in the rat facial nucleus following axotomy. J Neurosci 8:3181–3189.

Tso JY, Sun X-H, Kao T-H, Reece KS, Wu R (1985) Isolation and characterization of rat and human glyceraldehyde-3-phosphate dehydrogenase cDNAs: genomic complexity and molecular evolution of the gene. Nucleic Acids Res 13:2485–2502.

Vidal-Saenz M, Bray GM, Villegas-Perez MP, Thanos S, Aguayo AJ (1987) Axonal regeneration and synapse formation in the superior colliculus by retinal ganglion cells in the adult rat. J Neurosci 7:2894–2909.

Witt A, Brady ST (2000) Unwrapping new layers of complexity in axon/glial relationships. Glia 29:112–117.